Examining Neutrino Interactions with Quantum Kinetics and Quantum Information

Student: Sydney Stancik[1]
Mentors: Michael Cervia[2] and Vincenzo Cirigliano[1]

[1]Institute for Nuclear Theory, University of Washingtion, Seattle, WA 98195, USA

[2]Department of Physics, University of Washington, Seattle, WA 98195, USA

September 10, 2025

Abstract

Simulation of neutrino interactions in high energy astrophysical phenomena in principle is a many-body problem. Being able to map the propagation of a larger collection of these neutrinos can help us understand the dynamics and isotopic abundances resulting from nucleosynthetic processes in events like core-collapse supernova and neutron star mergers. Mapping neutrino oscillations in two different models, two-flavors and three-flavors, show, when considering neutrino-neutrino interactions, differing approximations of neutrino flavor abundance at different times. Moving forward, the many-body models of these astrophysical events will include the three known neutrino flavor states. Since this problem is a many-body one, to create meaningful simulations of these astrophysical events, in the future, larger systems of neutrinos must be taken into account.

1 The Neutrino

Neutrinos are chargeless particles whose interactions are mediated by weak force carriers, the W and Z bosons. Neutrinos are fermions, spin-$\frac{1}{2}$ particles, that exist within a large range of energies depending on the environments in which they are released [1]. The MeV scale will be considered in the following simulations of neutrino propagation. Neutrinos are leptons predicted by the Standard Model to have a flavor in association with the heavier leptons involved in their creation and annihilation processes. The mass of neutrinos with definite flavor has been found through the experiments of Super-Kamiokande [2] and Sudbury Neutrino Observatory [3] not to be definite. Due to the nature of these experiments, they determined that neutrinos of definite flavor are indeed massive only through a combination of mass states, which then results in oscillations of the neutrinos' flavor identity over time. Crucially, neutrinos oscillations were also found to be affected by matter through which they propagate, experimentally confirming the predicted Mikheev-Smirnov-Wolfenstein (MSW) effect [4]. For example, the core of the sun contains a sufficiently high electron density (10^{26} electrons/cm^3), such that the amplitude and frequency of the flavor oscillations of a solar neutrino can be altered measurably. The threshold for what is considered high density is determined relative to the energy and mass-squared difference of the neutrinos interacting with the matter.

Furthermore, understanding the evolution of an ensemble of neutrinos in time is useful in studying the various astrophysical processes in which they are involved. The thermodynamics of high energy processes like neutron star mergers and core-collapse supernovae, which produce neutrinos in extreme amounts (much greater than our Sun's luminosity in neutrinos), are hypothesized to be governed by these small, ultrarelativistic particles [1]. Determination of the frequencies at which these particles can change flavor can provide insight into the relative abundance of these particles at various stages of these astrophysical events. Stars live precariously in a balance between their own gravitational force keeping them compact and the pressure from their nucleosynthetic processes begging them to expand. As stars undergo nuclear fusion their gravitational force can overcome the pressure resulting in an explosive star death. Neutron star mergers, core-collapse supernovae, and early universe simulations are all high energy events where the abundance of neutrinos in these environments impacts the dynamics and nucleosynthesis of these environments. Neutrinos are responsible for the interchanging of entropy, energy, and lepton number in these events motivating our want of understanding the flavor evolution of a neutrino. Since these environments do not contain enough muon and tau leptons, the dominant process in neutrino transport is electron neutrino and antineutrino capture on nucleons [1].

$$\begin{aligned} \nu_e + n &\longleftrightarrow p + e^- \\ \bar{\nu}_e + p &\longleftrightarrow n + e^+ \end{aligned}$$

1.1 Neutrino Oscillations

Neutrino oscillations occur as neutrinos of definite flavor exist as a linear combination of three mass eigenstates and propagate through space. These states can be mapped via the Pontecorvo-Maki-Nakagawa-Sakata (PMNS) mixing matrix (U) where the matrix elements are parameterized by three mixing angles θ_{12}, θ_{23}, and θ_{13} and a CP-violating phase δ_{CP} [5]. These parameters govern the amplitude of the oscillations (i.e., the extent of flavor mixing), while the mass-squared difference between the eigenstates governs the frequency of the oscillations, as we shall soon demonstrate. Therefore, oscillation experiments in a vacuum inform us about the mass-squared difference values,

as opposed to absolute masses. Quantum mechanically, the measurable probability of neutrino flavor evolves in time, allowing the modeling of these flavor oscillations. Solving Schrodinger's equation for a neutrino requires the setup of a physically meaningful Hamiltonian. Note that the following equations are expressed in natural units so that $\hbar$ and c are set to 1.

The vacuum Hamiltonian in the flavor basis is

$$H_f \;=\; U H_m U^{\dagger}, \tag{1}$$

with

$$H_m \;\simeq\; \frac{1}{2E}\begin{pmatrix} 0 & 0 & 0 \\ 0 & \Delta m^2_{21} & 0 \\ 0 & 0 & \Delta m^2_{31} \end{pmatrix}.$$

where

$$E_i \;\approx\; p \;+\; \frac{m_i^2}{2p} \tag{2}$$

E_i is the energy of the ith neutrino mass state, where p is the neutrino momentum, and m_i is the mass state in question. The eigenvalues of the Hamiltonian express a relationship between the mass-squared difference and momentum of the neutrino, which in turn governs the frequency of these observable oscillations.

$$l_{mm'} \;=\; 2\pi\,\frac{2p}{|m^2 - m'^2|} \tag{3}$$

Determining the period at which these flavor oscillations occur from the probability allows for better predictions regarding the relative abundance of neutrinos of definite flavor at different points in time, particularly as they escape various sources. The rest of this section will present simple models to predict vacuum oscillations in two or three flavors.

1.1.1 Two-Flavor Model

The oscillations of neutrinos can be simplified in a two-flavor model where the neutrino can be of some flavor, say electron (or e), and another, say x, flavor where this x flavor is a combination of both the muon and tau flavors. This two-flavor approximation is sufficient in describing neutrino oscillations under many experimental conditions, when a mixing angle between any two mass states is negligible or the oscillation pattern is dominated by a single mass-squared difference [1]. An example of an environment meeting these conditions would be one in which the mixing of two flavors (μ and e) is maximized, resulting in the decoupling of tau flavor. In this case θ_{13} is very small and the oscillation frequency is determined by the Δm^2_{21}. The following two-dimensional mixing matrix describes these neutrinos (where in the specific case x would be μ).

$$\begin{pmatrix} \nu_e \\ \nu_x \end{pmatrix} = \begin{pmatrix} \cos\theta & \sin\theta \\ -\sin\theta & \cos\theta \end{pmatrix} \begin{pmatrix} \nu_1 \\ \nu_2 \end{pmatrix}$$

θ is the mixing angle, which determines the magnitude of the oscillations (how much flavor mixing can occur). These oscillations in probability, depicted in Fig. 1, are the vacuum flavor oscillations, in which a neutrino propagates undisturbed from other particles with which it can interact. Depending on the neutrino source, θ and Δm^2 require tuning to match those of a solar, atmospheric, or reactor neutrino. The oscillation lengths can be compared with the experimental data for each type of neutrino.

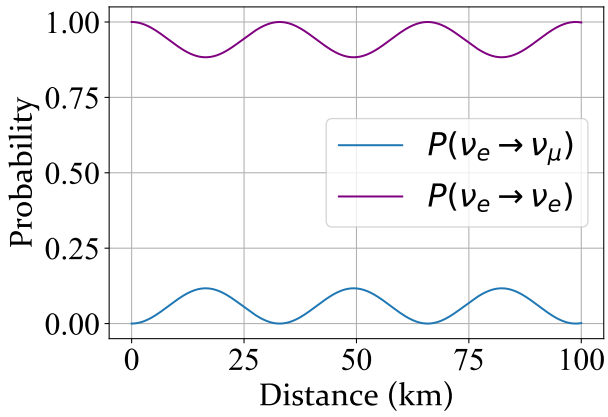

Figure 1: Probability of measuring a neutrino in a given flavor as it propagates in free space. Here consider a neutrino of momentum $p = 1$ MeV, mixing angle 10°, $\Delta m^2 = 7.53 \times 10^{-5}\text{eV}^2$, simulating a solar neutrino propagating through the vacuum with a small mixing.

1.1.2 Three-Flavor Model

These vacuum oscillations can also be modeled in three flavors, fully accounting for muon and tau neutrinos as well. The three-dimensional PMNS mixing matrix and two mass-squared differences allow the creation of the three-flavor Hamiltonian of a neutrino in a vacuum. Because the three-flavor model accounts for all three mass eigenstates, there are two independent mass-squared differences, and therefore two resulting independent frequencies from these vacuum oscillations. The interference pattern, of these frequencies, creates a wiggle on top of a wider, enveloping waveform, since our mass squared difference values between states 1 and 2 and 1 and 3 are different by a couple of orders of magnitude [6].

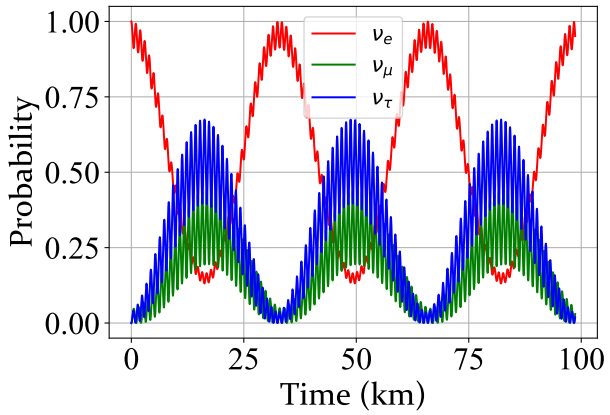

Figure 2: Same as in Fig. 1, but now consider a neutrino of momentum $p = 1$ MeV with two mass squared differences, $7.53 \times 10^{-5}\text{eV}^2$ (between masses 1 and 2) and $2.52 \times 10^{-3}\text{eV}^2$ (between masses 2 and 3). Here the mixing angles are $\theta_{12} = 33°$, $\theta_{23} = 49°$, $\theta_{13} = 9°$.

2 Modeling Neutrino Interactions

Neutrinos interact with quarks and leptons (including neutrinos) through the weak force. When neutrinos propagate through sufficiently dense matter, the interactions between these particles affect the frequency at which flavor oscillations occur. This phenomenon was first observed in detections of solar neutrinos, predicted by Wolfenstein [7] and then Mikheyev and Smirnov [4], implying that neutrinos' effective mass and mixing properties are affected by the environments through which they propagate.

Such drastic effects can arise from interactions of neutrinos with electrons as well as interactions of neutrinos with other neutrinos. In some high energy events the neutrino density is high enough (e.g., core-collapse supernovae) for neutrino-neutrino interactions to occur meaningfully. For simplicity we use coherent forward scattering to model these interactions [8], much like in the argument presented by Mikheev & Smirnov [4]. Coherent forward scattering follows similar assumptions of how photons interact with atoms here neutrinos elastically collide without changing directions, still allowing the coherent addition of the off-diagonal elements of the full interaction Hamiltonian. Neutrinos of definite momenta–ingoing and outgoing–experience flavor swaps, resulting in collective oscillations in flavor, due to these interactions beyond the vacuum.

2.1 Simulation of Matter Effects

When neutrinos propagate through matter, they most meaningfully interacting with electrons. In matter like on Earth' or our Sun, temperatures are too low for there to be enough of a presence of other neutrinos, muons, or taus for significant interactions to take place. The resulting effective one-body potential for each neutrino flavor is:

$$\begin{aligned} V_e &= \sqrt{2}\, G_F \left(n_e - \tfrac{n_n}{2}\right) \\ V_\mu &= \sqrt{2}\, G_F \left(n_\mu - \tfrac{n_n}{2}\right) \\ V_\tau &= \sqrt{2}\, G_F \left(n_\tau - \tfrac{n_n}{2}\right) \end{aligned} \tag{4}$$

where n_a is the number density of particle a and $G_f \sim 10^{-5}\text{GeV}^{-2}$ is the Fermi coupling constant. While neutrinos can interact with the quarks in protons and neutrons, the resulting change impacts all flavors of neutrinos, producing a global phase shift, which is not observed in flavor evolution. Moreover, neutrinos of only electron flavor interact directly with electrons at realistic energy scales, resulting in a relative phase difference between flavors, which can be seen in the time evolution of a neutrino propagating through matter. At low electron densities (like on Earth's surface for small distance scales) and energies (say, keV-MeV), the results of including the interaction potential, show no significant changes to the oscillations seen in the vacuum [1]. In contrast, at specific resonance densities, the oscillation length of these neutrinos can be set to its maximal value, following the MSW mechanism.

$$l_{\text{matter}} = \frac{l_{\text{vac}}}{\sqrt{\left(\cos(2\theta) - \frac{2\sqrt{2}G_F n_e p}{\Delta m^2}\right)^2 + \sin^2(2\theta)}} \tag{5}$$

This phenomena can be observed as neutrinos propagate in the Sun, where the electron density is so high at its core that oscillations are repressed. Then, when the neutrino reaches less compacted layers of the sun, the matter potential strength becomes equal to $\cos(2\theta)$ times the vacuum oscillation frequency, producing a lengthening effect on oscillations, which is followed a shortening of the oscillation length until the neutrino is propagating freely vacuum-like oscillation lengths [4]. I depict a simplified model of this behavior for two- and three-flavor models in Figs. 3 and 4, respectively.

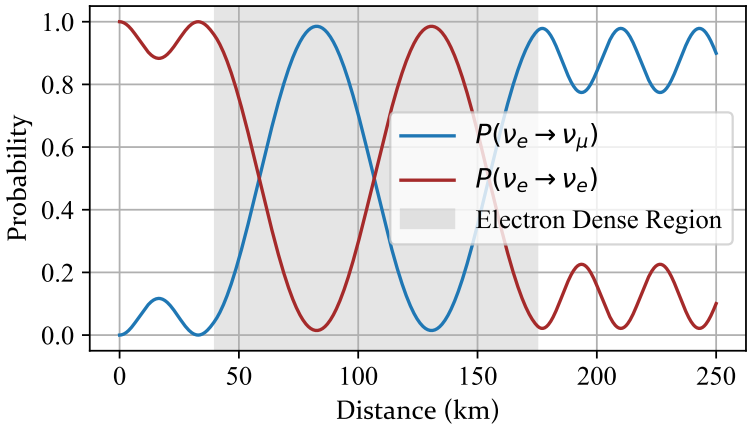

Figure 3: Evolution of a solar neutrino in two flavors, experiencing resonance when matter is "turned on" in the electron-dense region. The same parameters for vacuum oscillations were used as in Fig. 1, and the density for matter was taken to be 10^{26} electrons/cm^3.

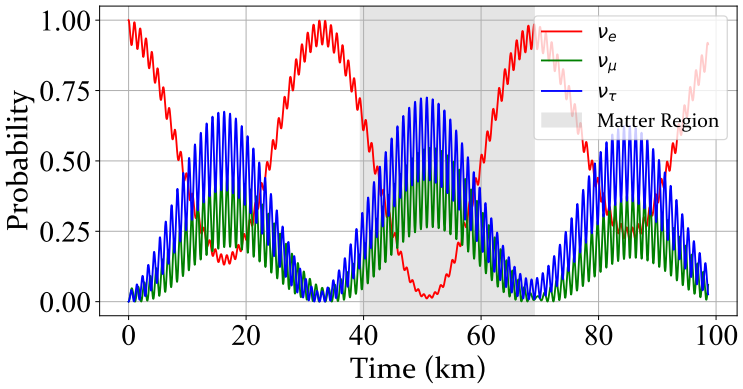

Figure 4: Evolution of a solar neutrino in three flavors, experiencing resonance when matter is "turned on" in an electron-dense region. The same parameters for vacuum oscillations were used as in Fig. 2, and the density for matter was taken to be 10^{26} electrons/cm^3.

This resonance electron density is determined by the energy, mass-squared differences, and (vacuum) mixing angles of the propagating neutrinos. Low-energy reactor neutrinos, say at 1 eV, can experience MSW effects at densities on par with that of Earth's core, an environment where atmospheric and solar neutrinos would not see much change in their oscillation periods or mixing amplitudes [9].

2.2 Simulation of Neutrino-Neutrino Interactions

In two-flavor modeling, the inclusion of neutrino-neutrino interactions results in higher energy oscillations. The period of flavor oscillations of the same solar neutrino went from vacuum oscillation lengths of 33 km to 9 km when only simulating the neutrino interaction. When including the vacuum oscillations an envelope forms where the faster interaction oscillations fell inside of the slower vacuum oscillations. To map these interactions in the three flavor model, two differing mass-squared values are used leading to the potential that these neutrino interactions might interfere with the faster vacuum oscillations creating more complicated flavor oscillations. These flavor oscillations lead to fluctuations in flavor abundance. The neutrino-neutrino interactions simulated in this research assume only coherent forward scattering. Non-forward scattering and wave packet size are computationally outside of the scope of this work thus far. To simulate neutrino-neutrino interactions, a potential term is added to the Hamiltonian:

$$H_{\nu\nu} = \mu(r)\,(1 - \cos(\theta_{ij})) \sum_{a=1}^{8} \lambda_a^{(i)} \otimes \lambda_a^{(j)} \tag{6}$$

where λ_a^i is the a-th Gell Mann matrix acting on the state of neutrino i, and θ_{ij} is the angle between momenta of neutrinos i and j. The neutrino interaction strength is directly related to the neutrino density of the environment that the neutrino is escaping. To simulate a physically intuitive situation the time dependence of the neutrino density must be taken into consideration. The changing neutrino strength in physical phenomena like core-collapse supernovae can be approximated as,

$$\mu(r) = \frac{G_F}{\sqrt{2}V}\left(1 - \sqrt{1 - \frac{R_\nu^2}{r^2}}\right)^2 \tag{7}$$

where V is a quantization volume, typically related to the neutrino number density, R_ν is a radius from which neutrinos are expected to start streaming freely, and r is the current radius to which the simulated neutrinos have propagated. The inclusion of these neutrino self interactions adds a third interfering frequency to the vacuum oscillations of a three flavor model, as shown in Fig. 5. To extract just the interaction collective oscillations, I plot results in the mass basis instead in Fig. 6. Since the mass basis experiences no oscillations in the vacuum (already eigenstates of the non-interacting Hamiltonian), the oscillations in the mass basis from this expanded Hamiltonian are a consequence of the neutrino-neutrino interaction exclusively.

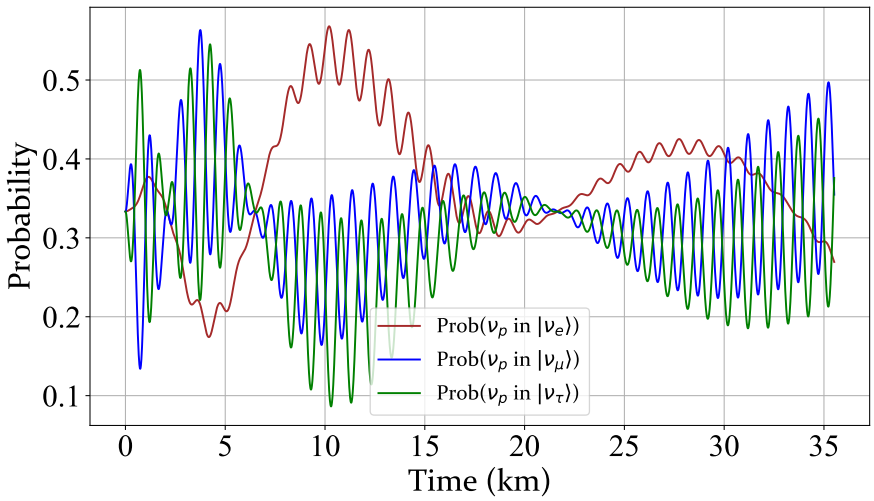

Figure 5: 1 MeV neutrino mapped in three flavors experiencing neutrino-neutrino interactions with a single other neutrino mode, escaping a neutrino gas with an interaction strength slowly and smoothly decreasing over time. The initial state of the simulation is: $\psi(0) = \frac{1}{\sqrt{3}}\big(\,|\nu_e\rangle \otimes |\nu_\mu\rangle \;+\; |\nu_\mu\rangle \otimes |\nu_\tau\rangle \;+\; |\nu_\tau\rangle \otimes |\nu_e\rangle\,\big)$. The initial interaction strength is, $\mu_0 = 10^{-3}$eV.

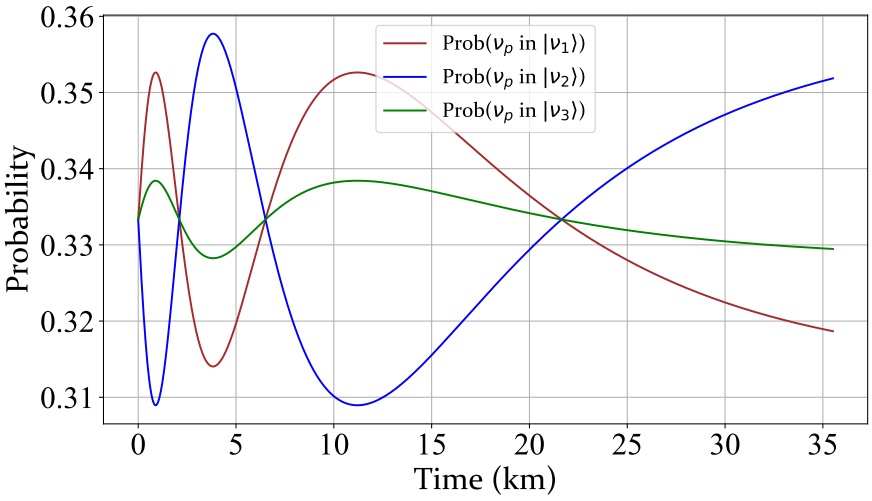

Figure 6: Same as in Fig. 5, but I plot probabilities of different mass eigenstates (instead of flavor eigenstates). As such, no vacuum oscillations are present, isolating effects of the neutrino-neutrino interaction at gradually decreasing densities.

2.2.1 Measuring Entanglement in Neutrino Interactions

When neutrinos interact with neutrinos, they can become entangled. The entanglement of a quantum system quantifies how (in)separable the quantum state of the system is. Particles in entangled systems evolve in time together to collectively form a state that does not reduce to a product of states describing each particle. Understanding how the entanglement of a neutrino system changes provides an insight into the state of the system and the relative flavor abundances.

Entanglement can be measured through the Von Neumann entropy of the system [10]. When the Von Neumann entropy is at its maximum, a system is considered to be maximally entangled. Von Neumann entropy can be found via,

$$S(p_i) = -\sum_i p_i \ln p_i \tag{8}$$

here p_i is the probability of an observable's eigenstate i, which can be extracted from the density matrix of the system. The density matrix of a pure state is given by,

$$\rho \equiv |\Psi\rangle\langle\Psi|, \tag{9}$$

while that of an impure, entangled state, is

$$\rho = \sum_i p_i \, |\Psi_i\rangle\langle\Psi_i|. \tag{10}$$

To map the entropy over time of a specific neutrino system in time involves separating the neutrinos by finding their reduced density matrix. The reduced density matrix keeps the evolved probabilities of flavor for the individual neutrino in question. These reduced density matrices can be found by tracing out the (quantum) degrees of freedom of all other neutrinos in the system (i.e., summing over the elements) [11],

$$\rho_n = \mathrm{Tr}_n[\rho] = \frac{1}{3}\left[\mathbb{I} + \frac{3}{2}\sum_j \lambda_j P_j\right]. \tag{11}$$

where ρ_n is the reduced density matrix of the nth neutrino, I is the 3×3 identity matrix and P_j are the components of the polarization vector of neutrino n.

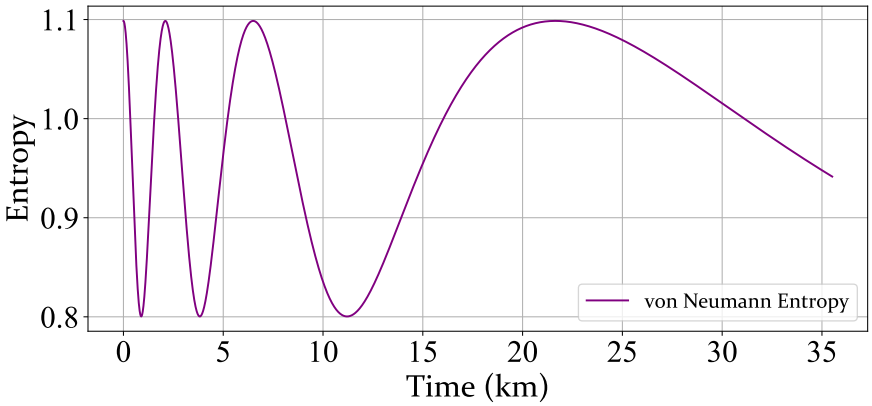

Figure 7: Entanglement entropy evolution of the same neutrino from Figs. 4 and 5. Note that the state of the system is pure but the neutrino in question is entangled with the other in the initial state; hence we see such oscillations in the purity (or equivalently, entropy) of the system. Since the system is modeled in three flavors the max entropy of the system is $\log(N_f)$ where N_f is the (quantum) degrees of freedom of the system [10]. Since the simulation was modeled using the natural log, the maximal entropy is $\ln(3)$.

3 Further Astrophysical Simulations

To simulate astrophysical events in which electron density and neutrino density will interplay in collective flavor oscillations, the two must be modeled together. Additionally, my future simulations of matter effects must treat them as time-dependent to map the escape of a neutrino from such an environment. In these extremely dense environments an appropriate approximation of the electron density must also be chosen. In these environments as well, there is more than just one escape path, so a many-body approach must be taken in order to simulate the evolution of these neutrinos, in order to fully account for the neutrino-neutrino interactions. Entanglement and entropy transport can then be modeled over time in these larger physical systems where N neutrinos are simulated.

3.1 Many-body Problems

Next steps in this research involve modeling these neutrino interactions as a many-body problem with more than two neutrinos in isolation. This goal requires creating a N-body Hamiltonian, the creation and separation of N-body density matrices, and time-efficient code, so that simulations can run feasibly. The many-body problem is considered as it is possible that the one-body treatment may not properly describe the dynamics of these high energy astrophysical events [12]. The many-body problem loses its triviality when the strength of the interaction terms is comparable to the scale of the neutrino as it results in a Hamiltonian that is difficult to approximate. In these scenarios, calculations beyond a mean-field approximation could result in a better description of these dynamics, as the mean-field approximation does not account for the quantum entanglement between neutrinos. Entanglement and entropy can affect the flavor content of neutrinos collectively,

so studying their evolution would strengthen our understanding of when nucleosynthetic processes can occur as well as energy transport via neutrinos.

Acknowledgement

This research was supported by the N3AS's National Science Foundation award No. 2020275. Thank you to the Institute of Nuclear Theory, University of Washington's INTURN program for this research opportunity.

References

[1] Carlo Giunti and Kim Chung Wook. *Fundamentals of Neutrino Physics and Astrophysics*. Oxford: Oxford Univ., 2007. DOI: 10.1093/acprof:oso/9780198508717.001.0001. URL: https://cds.cern.ch/record/1053706.

[2] Super-Kamiokande Collaboration et al. "Evidence for Oscillation of Atmospheric Neutrinos". In: *Physical Review Letters* 81.8 (Aug. 24, 1998). Publisher: American Physical Society, pp. 1562–1567. DOI: 10.1103/PhysRevLett.81.1562. URL: https://link.aps.org/doi/10.1103/PhysRevLett.81.1562.

[3] A. W. P. Poon. "Neutrino observations from the Sudbury Neutrino Observatory". In: *AIP Conference Proceedings* 610.1 (Apr. 2, 2002), pp. 218–230. ISSN: 0094-243X. DOI: 10.1063/1.1469931. URL: https://doi.org/10.1063/1.1469931 (visited on 08/27/2025).

[4] Stanislav P. Mikheev and A. Yu Smirnov. "Resonance oscillations of neutrinos in matter". In: *Soviet Physics Uspekhi* 30.9 (Sept. 1987), p. 759. DOI: 10.1070/PU1987v030n09ABEH002961. URL: https://dx.doi.org/10.1070/PU1987v030n09ABEH002961.

[5] Z. Maki, M. Nakagawa, and S. Sakata. "Remarks on the Unified Model of Elementary Particles". In: *Prog. Theor. Phys.* 28 (1962), pp. 870–880. DOI: 10.1143/PTP.28.870.

[6] S. Navas et al. "Review of particle physics". In: *Phys. Rev. D* 110.3 (2024), p. 030001. DOI: 10.1103/PhysRevD.110.030001.

[7] L. Wolfenstein. "Neutrino oscillations in matter". In: *Phys. Rev. D* 17 (9 1978), pp. 2369–2374. DOI: 10.1103/PhysRevD.17.2369.

[8] James Pantaleone. "Neutrino-neutrino forward scattering potentials". In: *Phys. Lett. B* 287 (1992), pp. 128–132. DOI: 10.1016/0370-2693(92)90757-7. arXiv: hep-ph/9206240 [hep-ph].

[9] E. Kh. Akhmedov. "Parametric resonance of neutrino oscillations and passage of solar and atmospheric neutrinos through the earth". In: *Nuclear Physics B* 538 (1999), pp. 25–51. DOI: 10.1016/S0550-3213(98)00723-8. arXiv: hep-ph/9805272 [hep-ph].

[10] Michael A. Nielsen and Isaac L. Chuang. *Quantum Computation and Quantum Information*. 10th Anniversary Edition. Cambridge: Cambridge University Press, 2010. ISBN: 978-1-107-00217-3. DOI: 10.1017/CBO9780511976667.

[11] Pooja Siwach, Anna M. Suliga, and A. Baha Balantekin. "Entanglement in three-flavor collective neutrino oscillations". In: *Phys. Rev. D* 107.2 (Jan. 2023). Publisher: American Physical Society, p. 023019. DOI: 10.1103/PhysRevD.107.023019. URL: https://link.aps.org/doi/10.1103/PhysRevD.107.023019.

[12] Michael J. Cervia et al. “Entanglement and collective flavor oscillations in a dense neutrino gas”. In: *Physical Review D* 100.8 (Oct. 2019). ISSN: 2470-0029. DOI: 10.1103/physrevd.100.083001. URL: http://dx.doi.org/10.1103/PhysRevD.100.083001.